

# Effect of retained austenite on the microstructure and mechanical properties of martensitic precipitation hardening stainless steel

H. NAKAGAWA\*, T. MIYAZAKI

*Department of Materials Science and Engineering, Nagoya Institute of Technology, Nagoya 466-8555, Japan*

The effect of retained austenite ( $\gamma$ ) on the microstructure and mechanical properties of a martensitic precipitation hardening stainless steel was experimentally investigated, whose chemical composition was Fe-1.8Cu-15.9Cr-7.3Ni-1.2Mo-0.08Nb-low C, N (mass %). The microstructures of all specimens consist of a typical lath martensite with interlath films of the retained  $\gamma$ , which is not reverted with aging. Cu-rich precipitates which may contribute to precipitation hardening can not clearly be observed. The tensile properties and Charpy absorbed energy are linearly approximated to the amount of retained  $\gamma$  as follows: 0.2% Y.S. (MPa) =  $1192.3 - 13.6 \times \gamma\%$ , T.S. (MPa) =  $1250.1 - 9.3 \times \gamma\%$ , El. (%) =  $12.16 + 0.43 \times \gamma\%$ , R.A. (%) =  $64.25 + 0.14 \times \gamma\%$ , and A.E. (J) =  $72.5 + 0.8 \times \gamma\%$ . The introduction of retained  $\gamma$  is not beneficial to the fatigue limit. An excellent combinations of strength, ductility and toughness obtained in the present work is attributed to the introduction of retained  $\gamma$  and also to the chemical composition of the specimen used.

© 1999 Kluwer Academic Publishers

## 1. Introduction

The improvement of the combinations of strength, ductility and toughness is one of the most important subjects on the development of steels. Moreover, high corrosion resistance is demanded for stainless steel.

High strength stainless steels of 1000 MPa grade tensile strength are mainly classified into the following four types: (1) martensitic precipitation hardening stainless steel, (2) low carbon martensitic stainless steel, (3) work hardening austenitic stainless steel, and (4) microduplex stainless steel. As for (1), many stainless steels such as 17-4 PH and PH 13-8 Mo stainless steels have been developed. These steels are usually aged at high temperature so as to have optimum combinations of strength, ductility and toughness. However, such heat treatment results in the lack of corrosion resistance. As for (2), some stainless steels having good toughness have been developed, however, these steels have lower corrosion resistance than others [1], since the additional amounts of Cr and Mo must be limited for the formation of a complete martensitic structure without  $\delta$ -ferrite phase. The (3) and (4) steels have excellent ductility and toughness [2]. However, the manufactured form of the steels is limited to plate shape due to the necessity of cold working, so that the (3) and (4) steels can not be utilized for shafts and bolts. On the basis of these conditions, the martensitic precipitation hardening stainless steel is considered to have a high

possibility for a better combination of strength, ductility, toughness and corrosion resistance without cold working.

The introduction of retained austenite ( $\gamma$ ) into martensitic steel is known to be one of the effective means for the improvements of toughness and ductility. The retained  $\gamma$  is effectively utilized in many kinds of steels, for example TRIP steel, 9% Ni steel and maraging steel. However, it is also known that the retained  $\gamma$  is not always effective and its validity has been often discussed. There are a few investigation about the effect of retained  $\gamma$  on martensitic precipitation hardening stainless steels [3–5], and there are fewer investigations on the positive use. The purpose of this study is to clarify the effect of retained  $\gamma$  on the microstructure and mechanical properties of martensitic precipitation hardening stainless steel.

## 2. Specimen and experimental procedure

### 2.1. Specimen

The chemical composition of the specimen used in the present work is shown in Table I. This composition was determined on the basis of some references [1, 6–10], and its detail will be described in Section 4.1. Fig. 1 shows the phase diagram calculated by the Thermo-Calc software [11]. When compared to Fe-Cr-Ni ternary phase diagram [12], Fig. 1 is found to have

\* Author to whom all correspondence should be addressed. H. Nakagawa, Department of Material Science and Engineering, Metals Section, Miyazaki Laboratory, Nagoya Institute of Technology, Gokiso-cho Showa-ku Nagoya 466-8555, Japan.

TABLE I Chemical composition of the specimen (mass %)

C	Cu	Ni	Cr	Mo	Nb	N	Fe
0.008	1.78	7.29	15.91	1.16	0.08	0.017	Bal.

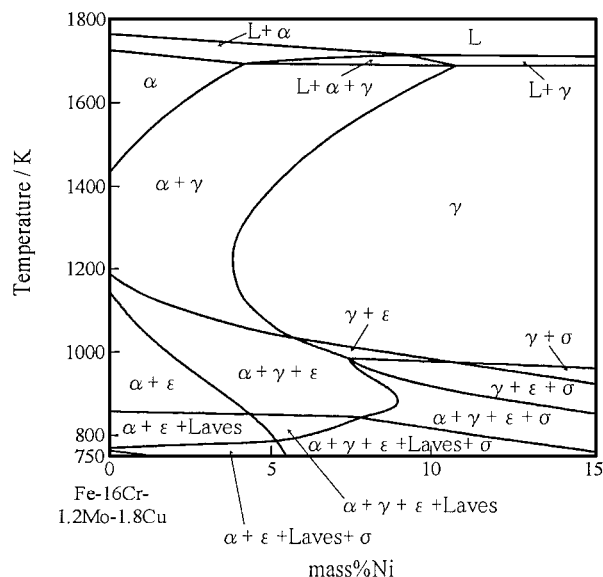


Figure 1 Phase diagram calculated by Thermo-Calc software.

Laves phase and  $\epsilon$ -Cu phase regions as a result of Mo and Cu additions, respectively.

The specimen was melted by using the multistage steelmaking process, and produced as rolled bars 80 mm in diameter by Aichi Steel Corporation for the purpose of minimizing non-metallic inclusions and impurities which affect its mechanical properties. Then they were hot forged as bars 15 mm in diameter. These bars were solution treated at 1373 K for 4.8 ks, quenched to various temperatures and then aged at 753 K for 14.4 ks. Three kinds of specimens containing about 10, 15 and 30% retained  $\gamma$ , respectively, were prepared by controlling the quenching temperature after solution treatment. Its detail will be described in Section 3.1.

## 2.2. Experimental

The heat treated specimens were examined by means of hardness test, X-ray diffraction technique, optical microscopy, transmission electron microscopy (TEM), and mechanical tests. The hardness test was performed on the tester set to the Rockwell C scale. The quantitative measurements of  $\gamma$  were determined by X-ray diffraction technique, where  $\text{CuK}\alpha$  in Rigaku X-ray diffractometer (Rint 1100) was used. The amounts of  $\gamma$  were estimated by the comparison of three peaks ( $(200)_{\text{bcc}}$ ,  $(211)_{\text{bcc}}$ ,  $(220)_{\text{bcc}}$  and  $(200)_{\text{fcc}}$ ,  $(220)_{\text{fcc}}$ ,  $(311)_{\text{fcc}}$ ) for each phase so as not to be affected by the preferred crystallographic orientation [13]. A reagent containing of 5 ml of hydrochloric acid, 4 g of picric acid and 100 ml of ethyl alcohol was used as the etchant for optical microscopy. For transmission electron microscopy the specimens were initially ground to a thick-

ness of 0.1 mm and were then electropolished at 288 K and at 15 V in an electrolyte containing 50 ml of perchloric acid and 450 ml of acetic acid. The thin foils were examined in a JEM 2000FX operating at 200 kV. The mechanical properties were evaluated by means of tensile test, Charpy impact test and rotating bending fatigue test. The tensile tests were performed on the round specimens with 40 mm in gauge length and 8 mm in gauge diameter. The crosshead speeds were 2 mm/min in the elastic range and 5 mm/min in the plastic range. The impact tests were performed on sub-size (10 by 5 mm) Charpy U-notch specimens (JIS Z 2202). The rotating bending fatigue tests were performed on unnotched round specimens with a diameter of 8 mm. After polishing the surface of the fatigue specimen by #800 emerypaper the fatigue test was carried out at a cycle speed of 3400 rpm. All mechanical tests were carried out at room temperature. Fractographic features were examined by means of scanning electron microscopy.

## 3. Experimental results

### 3.1. Control of the amount of retained austenite

In the present work, the amount of retained  $\gamma$  involved in specimens were adjusted by controlling the quenching temperature after solution treatment. Fig. 2 shows a process of the heat treatment. Specimens were quenched at various temperatures after solution treatment, and then aged at 753 K for 14.4 ks without cooling below each quenching temperature. Fig. 3 shows the effects of the quenching temperature on hardness and amount of  $\gamma$ . The specimens show same hardness of 38 HRC for quenching at 193 and 278 K but show the lower 35 HRC for quenching at higher temperature 333 K. On the retained  $\gamma$ , the specimens show just inverse behavior for the hardness; A good correlation between the hardness and the amount of  $\gamma$  is easily recognized. Consequently, the amount of retained  $\gamma$  involved in specimens were adjusted to about 10, 15 and 30% by controlling the quenching temperature at 278, 313 and 333 K, respectively.

The specimen as-quenched at 278 K had a hardness of 26 HRC and about 10% retained  $\gamma$ . Therefore, it is found that a hardness increment of 12 HRC was obtained with aging and also that the retained  $\gamma$  is not

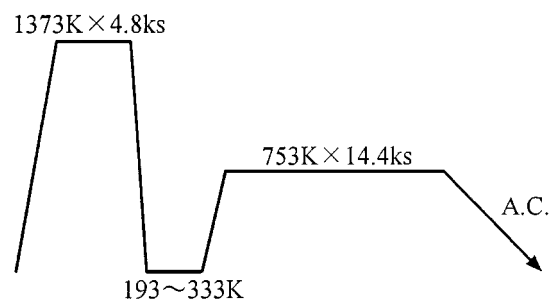


Figure 2 A process of the heat treatment. The specimens were water-quenched at each temperature after solution treatment. On quenching at 193 K the specimen was water-quenched, followed by the subzero treatment at 193 K. Each specimen was aged without cooling below each quenching temperature after solution treatment.

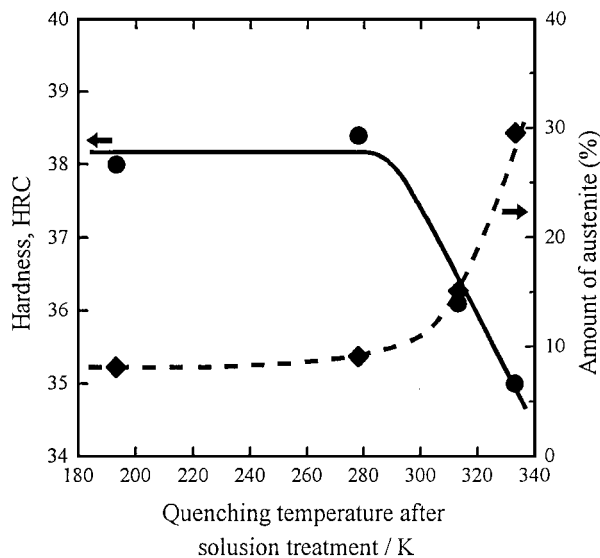


Figure 3 Effects of the quenching temperature on hardness and amount of austenite after aging at 753 K for 14.4 ks.

reverted with aging. Moreover, Fig. 3 reveals that the progress of martensitic transformation is delayed below 278 K, and about 10%  $\gamma$  remains even after subzero treatment at 193 K.

### 3.2. Observation of microstructure

Fig. 4 shows an optical micrograph of the specimen containing about 15% retained  $\gamma$ . The typical lath martensitic structure is recognized to be formed in a prior  $\gamma$  grain whose size is about 200  $\mu\text{m}$  in diameter. The difference of microstructure among the three kinds of specimens containing various  $\gamma$ -content can not be resolved by optical microscopy. The  $\delta$ -ferrite which exercises harmful influence on toughness was not observed, although Fig. 1 shows that the specimen should contain the  $\delta$ -ferrite after casting. Such  $\delta$ -ferrite may have been dissolved during the heating, rolling and forging.

The transmission electron micrographs of the specimen containing about 10% retained  $\gamma$  are shown in Fig. 5. The bright field image (Fig. 5a) shows a typ-

ical lath morphology of martensite containing a very high density of dislocation. The width of the laths is found to be 100–500 nm which is the same as some other experimental results [14, 15]. The dark field image (Fig. 5b) taken from  $\gamma$  reflection reveals the interlath films of retained  $\gamma$ . The selected area diffraction pattern (Fig. 5c) consists of two reciprocal lattice sections corresponding to bcc martensite and fcc  $\gamma$  as illustrated in Fig. 5d. This is consistent with the Nishiyama-Wassermann orientation relationship  $((011)_{\text{bcc}}//(\bar{1}\bar{1}\bar{1})_{\text{fcc}}, [100]_{\text{bcc}}//[110]_{\text{fcc}})$  [16–18]. However, it is difficult only from this result to determine the orientation relationship between the martensite and the  $\gamma$ . It is necessary to perform the accurate measurement of orientation relationship by tilting the specimen to the orientation  $[011]_{\text{bcc}}//[111]_{\text{fcc}}$  as indicated by Sandvik *et al.* [18]. The microstructures of the specimens containing about 15 and 30% retained  $\gamma$  were also observed by TEM. The retained  $\gamma$  between martensite laths were found to increase in amount and size with increasing retained  $\gamma$ . The twins formed on  $\{112\}_{\text{bcc}}$  plate were observed in all specimens, however, such the twins was very low in density.

Fig. 6 represents the transmission electron micrograph of the martensite lath shown in Fig. 5a. The precipitation hardening caused by Cu-rich precipitates, which transforms to incoherent  $\varepsilon$ -Cu phase by prolonged aging, was expected to occur in the present steel as same as in 17-4 PH stainless steel [19]. The precipitate particles can not clearly be observed because of a high density of dislocation in lath. However, many smaller precipitates are recognized to exist on the dislocations. Though Fig. 1 shows that  $\varepsilon$ -Cu, Laves and  $\sigma$  phases can exist at 753 K on equilibrium condition, the obtained precipitation hardening can be caused by Cu-rich precipitates, because Laves and  $\sigma$  phases were observed after long aging time [6], moreover, carbides and nitrides were not observed in all specimens.

### 3.3. Mechanical properties

Fig. 7 shows the effect of retained  $\gamma$  on the tensile properties. The 0.2% yield strength and tensile strength



Figure 4 Microstructure of the specimen quenched at 313 K after solution treatment and then aged at 753 K for 14.4 ks.

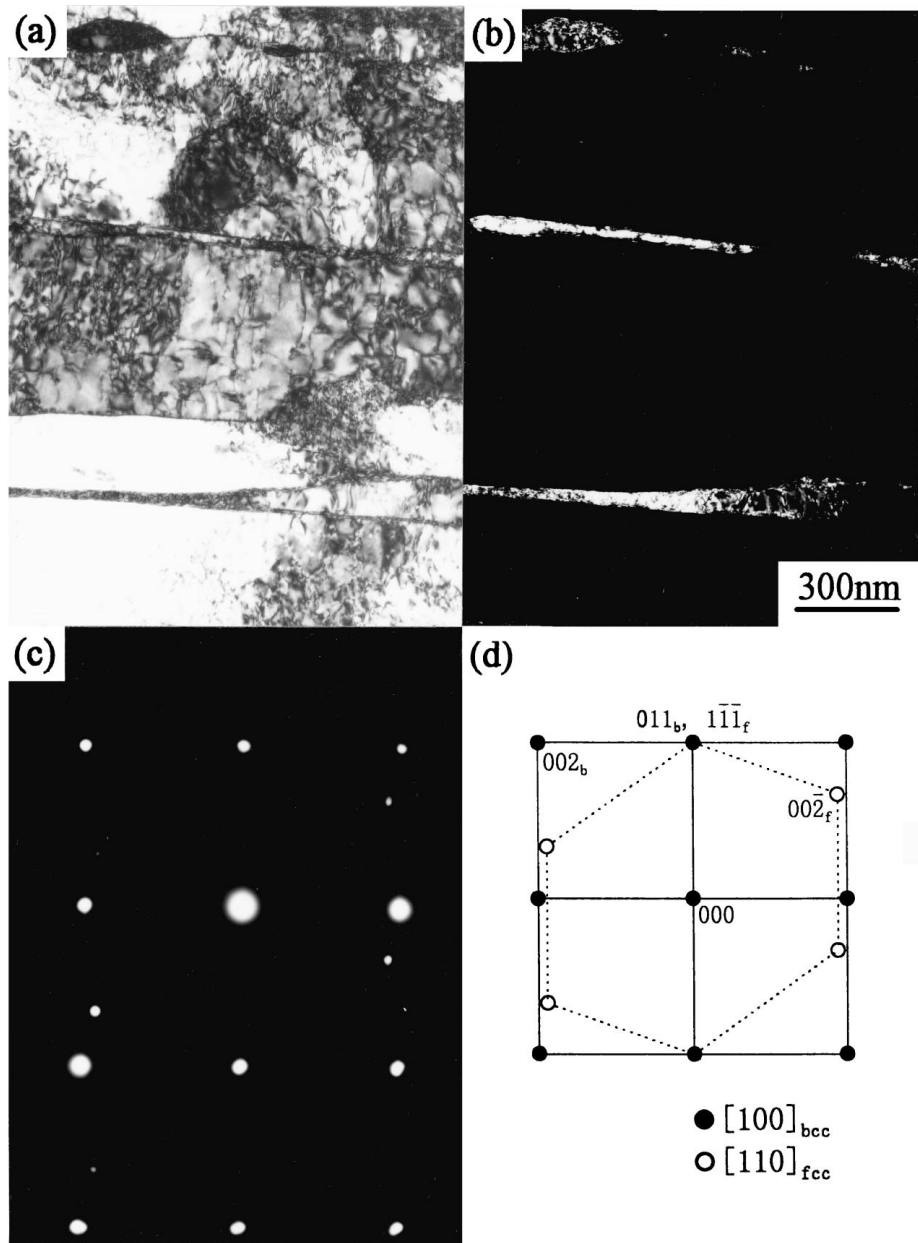


Figure 5 Transmission electron micrographs of the specimen quenched at 278 K after solution treatment and then aged at 753 K for 14.4 ks: (a) bright field image, (b) dark field image of retained austenite, (c) selected area diffraction pattern, and (d) schematic selected area diffraction pattern of (c).

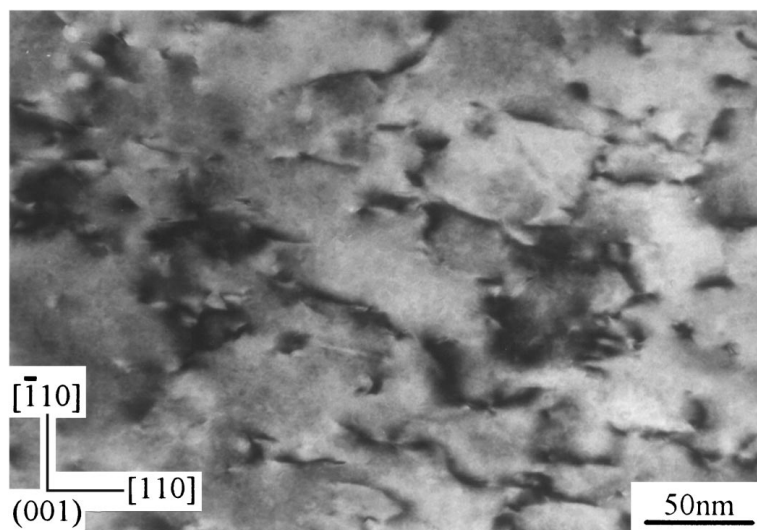


Figure 6 Transmission electron micrograph of the martensite lath shown in Fig. 5a.

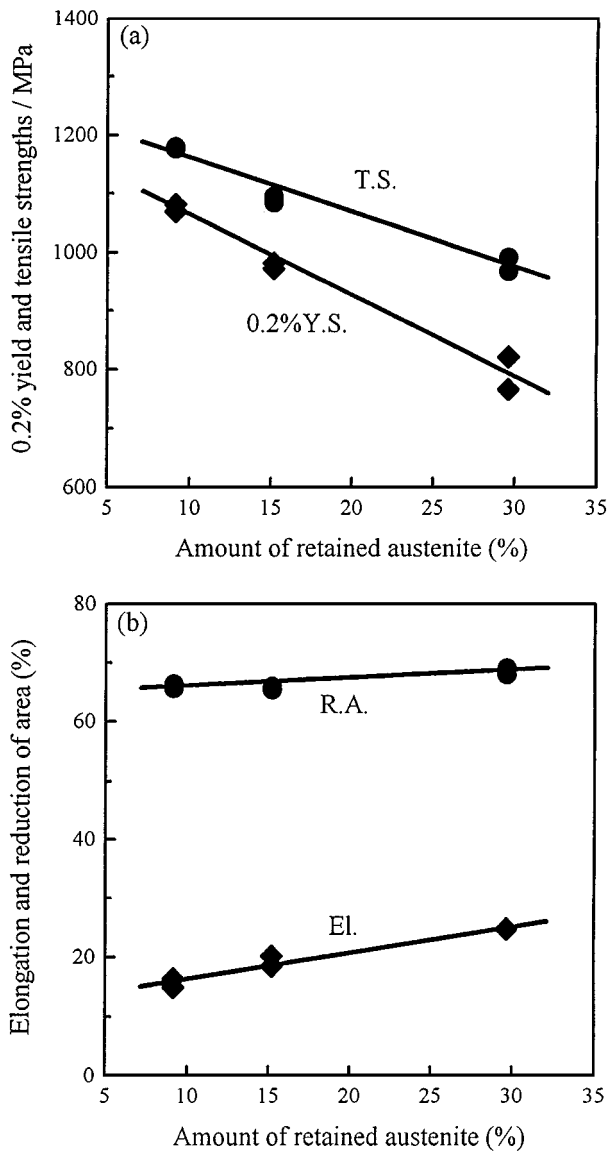


Figure 7 Effects of the amount of retained austenite on (a) the 0.2% yield and tensile strengths and (b) the elongation and reduction of area.

linearly decrease with increasing retained  $\gamma$ , while the elongation and reduction of area linearly increase. These behavior are approximately formulated to the amount of retained  $\gamma$  as follows:

$$0.2\% \text{ Yield Strength (MPa)} = 1192.3 - 13.6 \times \gamma\%$$

$$\text{Tensile Strength (MPa)} = 1250.1 - 9.3 \times \gamma\%$$

$$\text{Elongation (\%)} = 12.16 + 0.43 \times \gamma\%$$

$$\text{Reduction of Area (\%)} = 64.25 + 0.14 \times \gamma\%$$

X-ray diffraction just under the fracture surface of the tensile specimens proved that the retained  $\gamma$  in all specimens were completely transformed to martensite during tensile deformation.

Fig. 8 shows the effect of retained  $\gamma$  on the Charpy absorbed energy. The Charpy absorbed energy linearly rises with increasing retained  $\gamma$ , and the following linear approximation is obtained.

$$\text{Absorbed Energy (J)} = 72.5 + 0.8 \times \gamma\%$$

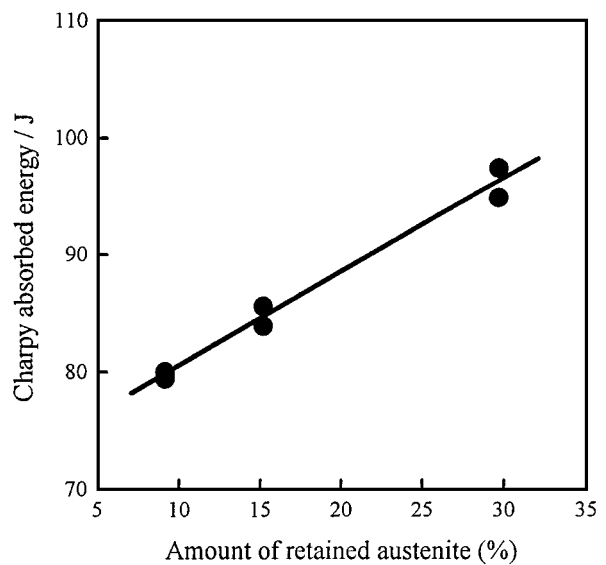


Figure 8 Effect of the amount of retained austenite on the Charpy absorbed energy.

The retained  $\gamma$  can be transformed to martensite around a crack-tip with stress concentration. In spite of the sub-size specimens, the obtained Charpy absorbed energies are very high values in the range 80–100 J. The fractographic feature of the impact specimen containing about 10% retained  $\gamma$  is shown in Fig. 9. Ductile dimpled fracture is observed with some aluminum oxides at the bottom of dimple. Similar dimpled fractures were observed in other specimens containing about 15 and 30% retained  $\gamma$ .

Fig. 10 shows the effect of retained  $\gamma$  on the fatigue limit evaluated by rotating bending fatigue test. The fatigue limit gradually decreases with increasing retained  $\gamma$ . The ratios between the fatigue limit and the tensile strength (fatigue limit/tensile strength) are 0.45, 0.46 and 0.50 for the specimen containing 10, 15 and 30% retained  $\gamma$ , respectively.

## 4. Discussion

### 4.1. Composition of specimen

For improving the ductility, toughness and corrosion resistance, the chemical composition of the specimen used in the present work was determined with the following three intentions: the reduction of carbides and nitrides, the reduction of  $\delta$ -ferrite content and the introduction of retained  $\gamma$ . In order to accomplish these intentions, it is necessary to lower C and N contents, to adjust the balance between the Cr-equivalent and the Ni-equivalent and to adjust  $M_s$  temperature.

Servant *et al.*, have reported that PH 17.4 Mo stainless steel (0.05C-15.95Cr-4.65Ni-1.24Mo steel, Z6 CND 17.04.02) consists of lath martensite with 18%  $\delta$ -ferrite after solution treatment and also that its  $M_s$  and  $M_f$  temperatures are 423 K and slightly higher than 293 K, respectively [6]. Nakazawa *et al.*, have reported that 0.5–2.0 mass % Mo addition improves the toughness of low carbon martensitic stainless steel [1]. The Mo addition is also generally known to be effective for corrosion resistance. In PH 17.4 Mo stainless steel lowering C content results in an increase in  $\delta$ -ferrite

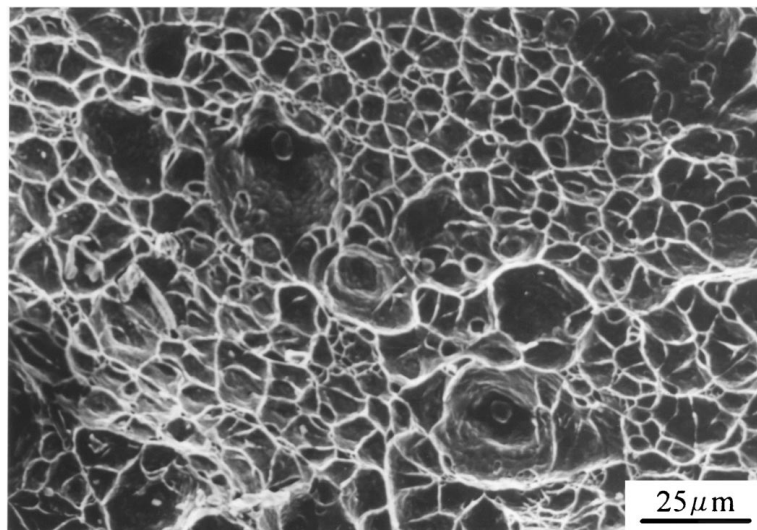


Figure 9 Fractographic feature of the Charpy impact specimen containing about 10% retained austenite.

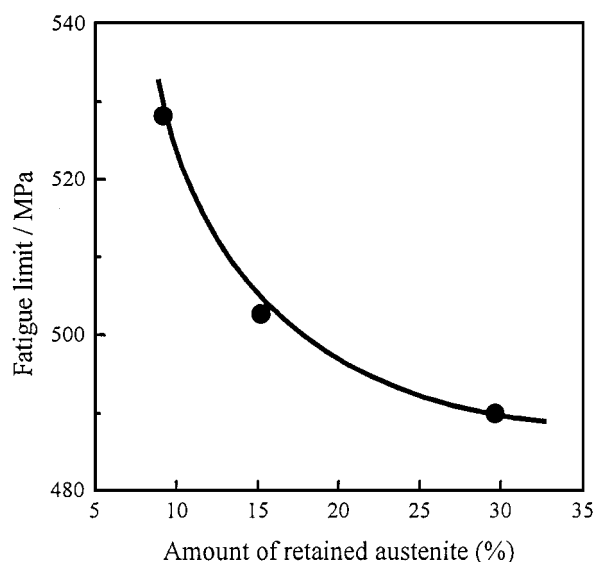


Figure 10 Effect of the amount of retained austenite on the fatigue limit.

content and a rise in  $M_s$  temperature. Therefore, proper amount of Ni, which is  $\gamma$  former and stabilizer in the same manner as C, was added for the purposes of reducing  $\delta$ -ferrite content and introducing retained  $\gamma$  on the basis of some references [7–10]. Moreover, 1.8 mass % Cu was added as a element for precipitation hardening. Finally, the chemical composition shown in Table I was determined. As a result of experiment, the specimen have no  $\delta$ -ferrite after solution treatment, and the amount of retained  $\gamma$  varied with the quenching temperature shown in Fig. 3.

#### 4.2. Stabilization of retained austenite

Two kinds of  $\gamma$  stabilization were observed in the present work. One is that the specimen quenched at 193 K has about 10% retained  $\gamma$  which is the same amount involved in the specimen quenched at 278 K. In the present work, the specimen containing low C and N contents was solution treated at high temperature for enough time, water quenched, and then immediately cooled to 193 K. Consequently, this stabilization of re-

tained  $\gamma$  may be attributed to the compression stress caused by the formation of 90% martensite during cooling [20, 21].

Another  $\gamma$  stabilization is that the  $\gamma$  introduced by quenching above room temperature, 313 and 333 K, do not transform to martensite during cooling after aging. However, since those  $\gamma$  contents before aging were not measured, it can not be confirmed that those retained  $\gamma$  did not transform at all during cooling. In the tempered martensitic steel containing Ni, the concentration of Ni content in reverted  $\gamma$  is known to chemically stabilize the  $\gamma$  [22, 23]. Though the reversion of  $\gamma$  with aging in the specimen quenched at 278 K could not be detected by X-ray diffraction technique as shown above, the possibility of concentration of Ni content in  $\gamma$  with aging can not be denied. Hence, the composition analyses of both martensite and  $\gamma$  phases were performed by using the specimen quenched at 333 K and then aged which had about 30% retained  $\gamma$ . The concentrations of main four elements, Fe, Cr, Ni and Mo, were analyzed by means of energy dispersive X-ray spectroscopy equipped in TEM. The concentration of Cu was not analyzed, because the error become larger due to the precipitation in the martensite. The total of concentrations of four elements was estimated to be 100 mass %. The results of composition analyses for both phases are presented in Table II. Though there are some scattering in measured values, there are no composition difference between the martensite and the  $\gamma$ , and the concentration of Ni content in the  $\gamma$  is not found. This result reveals that the chemical stabilization of  $\gamma$  does not occur. Consequently, the cause of this second stabilization of retained  $\gamma$  is considered to be the formation of atmospheres with interstitial atoms around lattice defects and the precipitation hardening of martensite [24].

#### 4.3. The effect of retained austenite on mechanical properties

As described in Section 3.3, the tensile properties were linearly approximated to the amount of retained  $\gamma$ , and the retained  $\gamma$  was found to be completely transformed

TABLE II Chemical compositions of the martensite and the retained austenite phases in the specimen quenched at 333 K after solution treatment and then aged at 753 K for 14.4 ks (mass %)

Element	Fe	Cr	Ni	Mo
Martensite phase	72.11	18.42	7.60	1.87
	75.00	16.43	7.63	0.94
	73.20	17.47	7.93	1.40
Retained austenite phase	74.02	16.85	7.85	1.28
	72.87	17.13	7.74	2.26

to martensite during tensile deformation. Since the retained  $\gamma$  is shown to be mechanically unstable [5, 14], 0.2% yield strength may appear due to the stress induced martensitic transformation of retained  $\gamma$ . On the other hand, tensile strength may depend on the phase ratio of the aging hardened martensite to the martensite formed with deformation. In addition, the martensitic transformation of retained  $\gamma$  during deformation may contribute to the improvement of elongation. Though this is explained as the TRIP effect in a wide sense, these specimens are inferior to the TRIP steel in a point of the effective use of retained  $\gamma$ . The product of tensile strength by elongation (T.S.  $\times$  El.) is often utilized as the index of the balance between the strength and the ductility. Its values are 18505, 21091 and 24353 (MPa%) for specimens containing about 10, 15 and 30% retained  $\gamma$ , respectively. The balance is found to be improved with increasing retained  $\gamma$ . It is in the same level as microduplex stainless steel [2] and low carbon martensitic stainless steels having good toughness [1], although inferior to work hardening austenitic stainless steel such as 301 type stainless steel.

The obtained high Charpy absorbed energies and observed ductile dimpled fractures may prove the attractive toughness of these specimens. The improvement of Charpy absorbed energy with increasing retained  $\gamma$  corresponds to the decrease of strength. In addition, the martensitic transformation of retained  $\gamma$  with a crack propagation may also contribute to the improvement of the toughness.

These results support that the introduction of retained  $\gamma$  is effective means for the improvements of ductility and toughness of martensitic precipitation hardening stainless steel. Moreover, the chemical composition of the specimen used in this work is also attributed to those improvements.

There are many investigations about the effect of retained  $\gamma$  on the fatigue property of many steels [25–27]. However, there is no agreed point of view whether retained  $\gamma$  is effective for fatigue property or not. The result of fatigue tests shown in Fig. 10 suggests that the introduction of retained  $\gamma$  is not beneficial to the fatigue limit.

## 5. Conclusion

The effect of retained  $\gamma$  on the microstructure and mechanical properties was investigated for a martensitic precipitation hardening stainless steel, whose chemical composition was Fe-1.8Cu-15.9Cr-7.3Ni-1.2Mo-0.08Nb-low C, N (mass%). The amount of retained  $\gamma$

was adjusted by controlling the quenching temperature after solution treatment. The main results obtained are as follows:

1. Microstructures of all specimens consist of a typical lath martensite with interlath films of the retained  $\gamma$ , which is not reverted with aging. Cu-rich precipitates which may contribute to precipitation hardening can not clearly be observed.

2. The tensile properties and Charpy absorbed energy are linearly approximated to the amount of retained  $\gamma$  as follows:

$$0.2\% \text{ Yield Strength (MPa)} = 1192.3 - 13.6 \times \gamma\%$$

$$\text{Tensile Strength (MPa)} = 1250.1 - 9.3 \times \gamma\%$$

$$\text{Elongation (\%)} = 12.16 + 0.43 \times \gamma\%$$

$$\text{Reduction of Area (\%)} = 64.25 + 0.14 \times \gamma\%$$

$$\text{Absorbed Energy (J)} = 72.5 + 0.8 \times \gamma\%$$

The introduction of retained  $\gamma$  is not beneficial to the fatigue limit.

3. The balance between the strength and the ductility is improved with increasing retained  $\gamma$ . It is in the same level as microduplex stainless steel and low carbon martensitic stainless steels having good toughness, although inferior to work hardening austenitic stainless steel. An excellent combinations of strength, ductility and toughness obtained in the present work is attributed to the introduction of retained  $\gamma$  and also to the chemical composition of the specimen used.

## Acknowledgement

The author would like to thank H. Yokota in Aichi Steel Corporation for the preparation of specimen and helpful advice.

## References

1. T. NAKAZAWA, M. TENDO, Y. SATO, Y. TADOKORO, H. OUCHI, H. INOUE, H. SAKURAI and K. SUETSUGU, *Shinittetu Gihō* **361** (1996) 36 (in Japanese).
2. Y. MURATA, S. OHASHI and Y. UEMATSU, *Tetsu-to-Hagane* **78** (1992) 346 (in Japanese).
3. D. WEBSTER, *Trans. ASM* **61** (1968) 816.
4. *Idem.*, *Metall. Trans.* **2** (1971) 2097.
5. W. M. GARRISON, JR. and J. A. BROOKS, *Mater. Sci. Eng.* **A149** (1991) 65.
6. C. SERVANT, E. H. GHERBI and G. CIZERON, *J. Mater. Sci.* **22** (1987) 2297.
7. W. T. DELONG, *Metal Prog.* **77** (1960) 98.
8. L. PRYCE and K. W. ANDREWS, *JISI* **195** (1960) 415.
9. K. J. IRVINE, D. T. LLEWELLYN and F. B. PICKERING, *ibid.* **194** (1959) 218.
10. K. ISHIDA, *J. Alloys Comp.* **220** (1995) 126.
11. B. SUNDMAN, B. JANSSON and J. O. ANDERSSON, *CALPHAD* **9** (1985) 153.
12. M. HILLERT and C. QUI, *Metall. Trans. A* **21A** (1990) 1673.
13. M. J. DICKSON, *J. Appl. Cryst.* **2** (1969) 176.
14. V. SEETHARAMAN, *Mater. Sci. Eng.* **47** (1981) 1.
15. M. MAKI, K. MORIMOTO and I. TAMURA, *Trans. ISIJ* **20** (1980) 700.
16. B. V. N. RAO, *Metall. Trans. A* **10A** (1979) 645.
17. Y. KATZ, H. MATHIAS and S. NADIV, *ibid.* **14A** (1983) 801.

18. B. P. J. SANDVIK and C. M. WAYMAN, *ibid.* **14A** (1983) 809.
19. U. K. VISWANATHAN, *Mater. Sci. Eng.* **A104** (1988) 181.
20. B. V. N. RAO and G. THOMAS, in Proceedings of the 3rd International Conference on Martensitic Transformations, Boston, 1979, edited by W. S. Owen (MIT Press, Cambridge) p. 12.
21. H. K. D. H. BHADESHIA and D. V. EDMONDS, in Proceedings of the 3rd International Conference on Martensitic Transformations, Boston, 1979, edited by W. S. Owen (MIT Press, Cambridge) p. 28.
22. W. SHA, A. CEREZO and G. D. W. SMITH, *Metall. Trans. A* **24A** (1993) 1221.
23. P. P. SINHA, D. SIVAKUMAR, N. S. BABU, K. T. THARIAN and A. NATARAJAN, *Steel Res.* **66** (1995) 490.
24. H. SUDO and T. YAMAGATA, *J. Japan Inst. Metals* **34** (1970) 968 (in Japanese).
25. H. E. FRANKEL, J. A. BENNETT and W. A. PENNINGTON, *Trans. ASM* **52** (1959) 257.
26. R. O. RITCHIE, V. A. CHANG and N. E. PATON, *Fatigue Eng. Mater. Struct.* **1** (1979) 107.
27. H. J. CHOI and L. H. SCHWARTZ, *Metall. Trans. A* **14A** (1983) 1089.

*Received 23 September 1998  
and accepted 11 February 1999*